有界面之毛細流體問題之數學模型與數值計算
期中報告

賴明治

中文摘要：

在這篇報告中，我們將原先在二維所發展出來針對有界面活性劑的流體數值模擬，推廣至三維軸對稱的問題上面。其中的主要差異是 (1) 因計算區域及座標的不同，所以 Navier-Stokes 算法的不同，(2) 界面力的不同，(3) 加上在界面均勻網格的機制。我們的數值方法仍然保有界面活性劑總質量守恆的特性，我們也模擬了單一液滴在延展流的物理行為，所得結果與其它文獻結果類似。

關鍵詞：內嵌邊界法、軸對稱界面、Navier-Stokes 方程、界面活性劑。

英文摘要：

In this paper, we extend our previous work on the two-dimensional immersed boundary method for interfacial flows with insoluble surfactant to the case of three-dimensional axisymmetric interfacial flows. Although the key components of the scheme are similar in spirit to the two-dimensional case, there are two differences introduced in the present work. Firstly, the governing equations are written in an immersed boundary formulation using the axisymmetric cylindrical coordinates. Secondly, we introduce an artificial tangential velocity to the Lagrangian markers so that the uniform distribution of markers along the interface can be achieved and a modified surfactant concentration equation is derived as well. The numerical scheme still preserves the total mass of surfactant along the interface. Numerical convergence of the present scheme has been checked, and several tests for a drop in extensional flows have been investigated in detail.

Keywords: Immersed boundary method; Axisymmetric interfacial flow;
Navier-Stokes equations; Surfactant

INTERNATIONAL JOURNAL OF
NUMERICAL ANALYSIS AND MODELING
Volume 00, Number 0, Pages 000–000

SIMULATING THE AXISYMMETRIC INTERFACIAL FLOWS WITH INSOLUBLE SURFACTANT BY IMMERSED BOUNDARY METHOD

MING-CHIH LAI, CHUNG-YIN HUANG AND YI-MIN HUANG

Abstract. In this paper, we extend our previous work on the two-dimensional immersed boundary method for interfacial flows with insoluble surfactant to the case of three-dimensional axisymmetric interfacial flows. Although the key components of the scheme are similar in spirit to the two-dimensional case, there are two differences introduced in the present work. Firstly, the governing equations are written in an immersed boundary formulation using the axisymmetric cylindrical coordinates. Secondly, we introduce an artificial tangential velocity to the Lagrangian markers so that the uniform distribution of markers along the interface can be achieved and a modified surfactant concentration equation is derived as well. The numerical scheme still preserves the total mass of surfactant along the interface. Numerical convergence of the present scheme has been checked, and several tests for a drop in extensional flows have been investigated in detail.

Key Words. Immersed boundary method; Axisymmetric interfacial flow; Navier-Stokes equations; Surfactant

1. Introduction

Surfactant are surface active agents that adhere to the fluid interface and affect the interface surface tension. Surfactant play an important role in many applications in the industries of food, cosmetics, oil, etc. For instance, the daily extraction of ore rely on the subtle effects introduced by the presence of surfactant [6]. In a liquid-liquid system, surfactant allow small droplets to be formed and used as an emulsion. Surfactant also play an important role in water purification and other applications where micro-sized bubbles are generated by lowering the surface tension of the liquid-gas interface. In microsystems with the presence of interfaces, it is extremely important to consider the effect of surfactant since in such cases the capillary effect dominates the inertia of the fluids [21]. In bio-mechanical flows, for example, some insects drift on the water by injecting a chemical excretion at the rear to reduce the surface tension behind their bodies such that the insects are pulled forward.

In [11], we develop an immersed boundary method for two-dimensional interfacial flows with insoluble surfactant. In this paper, we extend our previous work to the three-dimensional axisymmetric case where the governing equations are written in immersed boundary formulation [16]. Other related works on the simulations for axisymmetric interfacial flows with insoluble surfactant using different methodology

2000 *Mathematics Subject Classification.* 65M06, 76D45.

This research was supported in part by National Science Council of Taiwan under research grant NSC-97-2628-M-009-007-MY3 and MoE-ATU project.

including the boundary integral method, volume-of-fluid method, front-tracking method, and the arbitrary Lagrangian Eulerian method can be found in [20, 18, 23, 9, 12, 7, 5], just to name a few. The simulations for axisymmetric interfacial flows with soluble surfactant using the front-tracking method can refer to [25, 15, 24].

For simplicity, we consider an axisymmetric drop immersed in a viscous incompressible fluid. We also assume that the fluids inside and outside of the drop are the same, and they are governed by the incompressible Navier-Stokes equations. Under the axisymmetric assumption, one can describe the drop interface Σ with a parametric form $\mathbf{X}(s,t) = (R(s,t), Z(s,t)), 0 \le s \le 2\pi$, where s is the parameter of the initial configuration of the interface. Note that, s is not necessarily the arc-length parameter. The unit tangent vector $\boldsymbol{\tau}$ and the outward normal vector $\mathbf{n}$ on the interface can be defined as

$$\boldsymbol{\tau}(s,t) = \frac{\boldsymbol{X}_s}{|\boldsymbol{X}_s|} = \frac{(R_s, Z_s)}{\sqrt{R_s^2 + Z_s^2}}, \qquad \mathbf{n} = \frac{(Z_s, -R_s)}{\sqrt{R_s^2 + Z_s^2}}, \tag{1.1}$$

respectively, where the subscript denotes the partial derivative with respect to s.

Under the assumption of axis-symmetry, the 3D Navier-Stokes equations can be simply written in a 2D manner using the axisymmetric cylindrical coordinates $\mathbf{x} = (r, z)$. Throughout this paper, we denote $\boldsymbol{u} = (u, w)$ as the velocity defined on a 2D meridian domain $\Omega = \{(r,z) | 0 < r \le a, c \le z \le d\}$, where u and w are the radial (r coordinate) and axial (z coordinate) velocity components. We also denote $\boldsymbol{U} = (U, W)$ as the corresponding velocity component on the interface. The non-dimensional Navier-Stokes equations are

$$\frac{\partial u}{\partial t} + u\frac{\partial u}{\partial r} + w\frac{\partial u}{\partial z} + \frac{\partial p}{\partial r} = \frac{1}{Re}(\Delta u - \frac{u}{r^2}) + \frac{1}{ReCa} f_r \tag{1.2}$$

$$\frac{\partial w}{\partial t} + u\frac{\partial w}{\partial r} + w\frac{\partial w}{\partial z} + \frac{\partial p}{\partial z} = \frac{1}{Re}\Delta w + \frac{1}{ReCa} f_z \tag{1.3}$$

$$\frac{1}{r}\frac{\partial}{\partial r}(ru) + \frac{\partial w}{\partial z} = 0 \tag{1.4}$$

where the Laplacian operator is defined as

$$\Delta = \frac{1}{r}\frac{\partial}{\partial r}\left(r\frac{\partial}{\partial r}\right) + \frac{\partial^2}{\partial z^2}. \tag{1.5}$$

For later convenience, we introduce the gradient and divergence operators as

$$\nabla = \left(\frac{\partial}{\partial r}, \frac{\partial}{\partial z}\right) \qquad \tilde{\nabla}\cdot = \left(\frac{1}{r}\frac{\partial}{\partial r} r, \frac{\partial}{\partial z}\right)\cdot. \tag{1.6}$$

Thus, the Laplace operator can be written as $\Delta = \tilde{\nabla} \cdot \nabla$.

The fluid-interface interaction equations can be written as

$$\boldsymbol{f} = (f_r, f_z) = \int_0^{2\pi} \mathbf{F}(s,t)\, \delta^2(\mathbf{x} - \mathbf{X}(s,t))\, ds, \tag{1.7}$$

$$\mathbf{F}(s,t) = \frac{\partial}{\partial s}(\sigma\, \boldsymbol{\tau}) - \frac{Z_s}{R}\, \sigma\, \mathbf{n} \tag{1.8}$$

$$\frac{\partial \mathbf{X}(s,t)}{\partial t} = \boldsymbol{U}(s,t) = \int_\Omega \boldsymbol{u}(\mathbf{x},t)\, \delta^2(\mathbf{x} - \mathbf{X}(s,t))\, d\mathbf{x}. \tag{1.9}$$

One can immediately see that interfacial force $\mathbf{F}(s,t)$ is slightly different from the two-dimensional counterpart since an extra term is added. A detailed derivation for Eq. (1.8) is given in the Appendix. Notice that, the above immersed boundary formulation is also used in [25].

The dimensionless numbers are the Reynolds number Re describing the ratio between the inertial force and the viscous force, and the capillary number Ca describing the strength of the surface tension. Equations (1.7)-(1.9) represent the interaction between the immersed interface and the fluids. In particular, Eq. (1.7) describes the force $\mathbf{f}$ acting on the fluid due to the interfacial force $\mathbf{F}$, which is basically the effect of surface tension σ as in Eq. (1.8). Eq. (1.9) states that the interface moves with the fluid velocity. The present formulation employs a mixture of Eulerian ($\mathbf{x} = (r, z)$) and Lagrangian ($\mathbf{X} = (R, Z)$) variables which are linked by the two-dimensional Dirac delta function $\delta^2(\mathbf{x}) = \delta(r)\delta(z)$.

The surface tension σ is related to the surfactant concentration Γ through the dimensionless Langmuir model [1]

$$\sigma = \sigma_c(1 + \ln(1 - \beta\,\Gamma), \tag{1.10}$$

where σ_c is the surface tension without surfactant, and β is the elasticity number representing the sensitivity between the surfactant and the surface tension. In order to close the system, we still need one more equation for surfactant concentration evolution. As mentioned before, surfactant are insoluble to the buck fluids, so they are simply convected and diffused along the interface. Since there is no exchange between the interface and the bulk fluids, the total mass of the surfactant must be conserved. As derived in [19, 22], the dimensionless surfactant concentration equation is

$$\frac{D\Gamma}{Dt} + (\nabla_s \cdot \boldsymbol{u})\,\Gamma = \frac{1}{Pe_s}\,\nabla_s^2\Gamma, \tag{1.11}$$

where $\frac{D}{Dt}$ is the material derivative, ∇_s and ∇_s^2 are the surface gradient and surface Laplacian operators respectively. The dimensionless number Pe_s is called the surface Peclet number that represents the diffusion coefficient of the surfactant along the interface. In axisymmetric form, Eq. (1.11) can be written as by

$$\frac{D\Gamma}{Dt} + (\nabla_s \cdot \boldsymbol{u})\,\Gamma = \frac{1}{Pe_s}\,\frac{1}{R\,|\boldsymbol{X}_s|}\,\frac{\partial}{\partial s}\left(\frac{R}{|\boldsymbol{X}_s|}\,\frac{\partial\Gamma}{\partial s}\right). \tag{1.12}$$

One way to derive the surface divergence $\nabla_s \cdot \boldsymbol{u}$ is as follows. Let the differential element of surface dS in axisymmetric coordinates be $dS = R|\boldsymbol{X}_s|$. Then, we have

$$\begin{aligned}\frac{\partial dS}{\partial t} &= \frac{\partial}{\partial t}\left(R|\boldsymbol{X}_s|\right) = \frac{\partial R}{\partial t}|\boldsymbol{X}_s| + R\frac{\partial|\boldsymbol{X}_s|}{\partial t} = U|\boldsymbol{X}_s| + R\frac{\boldsymbol{X}_s\cdot\boldsymbol{X}_{s,t}}{|\boldsymbol{X}_s|}\\ &= U|\boldsymbol{X}_s| + R\frac{\boldsymbol{X}_s\cdot\boldsymbol{U}_s}{|\boldsymbol{X}_s|} = U|\boldsymbol{X}_s| + R\frac{\partial\boldsymbol{U}}{\partial s}\cdot\boldsymbol{\tau} = \left(\frac{U}{R} + \frac{\partial\boldsymbol{U}}{\partial\boldsymbol{\tau}}\cdot\boldsymbol{\tau}\right)R|\boldsymbol{X}_s|\end{aligned}$$

By using the fact that $\frac{\partial dS}{\partial t} = (\nabla_s \cdot \boldsymbol{u})\,dS$ in [2], one can easily conclude that the surface divergence

$$\nabla_s \cdot \boldsymbol{u} = \frac{U}{R} + \frac{\partial\boldsymbol{U}}{\partial\boldsymbol{\tau}}\cdot\boldsymbol{\tau} \tag{1.13}$$

We can also see that the surface divergence of the velocity only involves the velocity value on the interface. Another similar form for the above surfactant convective-diffusion equation that is written involving the tangential velocity component, the normal velocity component, and the interface curvature can be found in [20].

2. An equi-distributed technique for Lagrangian markers

In the context of immersed boundary simulations, the interface is tracked in a Lagrangian manner. Once the Lagrangian markers have been chosen initially, the movement of those markers are based on the interpolated local fluid velocity as

shown in Eq. (1.9). Very often, as time evolves, those Lagrangian markers will be either clustered together or dispersed so the overall numerical stability or accuracy can be compromised. Therefore, certain grid equi-distributed technique must be adopted to preserve better resolution. One approach is to add or delete marker points, when they are needed or unwanted, as shown in our previous immersed boundary simulation for a drop in a shear flow [11], where the marker points are gradually swept into the tips region. In this paper, we introduce another convenient way to control the Lagrangian markers by implementing an equi-distributed technique along the interface. One should notice that a similar particle equi-distribution can be found in [4]. However, the present form is simpler than the one in [4] since there is no need to calculate the curvature.

In order to remove the stiffness from the interfacial flows with surface tension, Hou, Lowengrub and Shelly [8] introduced an artificial tangential velocity into their formulation of boundary integral methods so that the particles can be uniformly distributed. Following [8], we propose the following technique to maintain an equi-distribution of the Lagrangian markers.

The idea is to introduce an artificial tangential velocity, $\bar{U}$, to the marker so that the marker $\mathbf{X}(s,t)$ satisfies $|\boldsymbol{X}_s|_s = 0$. Let

$$\frac{\partial \mathbf{X}}{\partial t} = \mathbf{U}(s,t) + \bar{U}(s,t)\,\boldsymbol{\tau} = \int_\Omega \mathbf{u}(\mathbf{x},t)\,\delta^2(\mathbf{x}-\mathbf{X}(s,t))d\mathbf{x} + \bar{U}(s,t)\,\boldsymbol{\tau} \tag{2.14}$$

Let $L_s = |\boldsymbol{X}_s|$, then we have $L_{s,s} = 0$ which implies that L_s is independent of s and dependent on t so we can write

$$L_s(t) = \frac{1}{2\pi}\int_0^{2\pi} L_{s'}(s',t)\,ds'. \tag{2.15}$$

By taking the time derivative, we have

$$L_{s,t}(t) = \frac{1}{2\pi}\int_0^{2\pi} L_{s',t}(s',t)\,ds'. \tag{2.16}$$

One can write out the time derivative of the stretching factor explicitly as

$$\begin{aligned} L_{s,t} &= \frac{\partial}{\partial t}|\boldsymbol{X}_s| = \frac{\partial}{\partial t}\sqrt{R_s^2+Z_s^2} = \frac{1}{2}\left(R_s^2+Z_s^2\right)^{-1/2}(2R_sR_{st}+2Z_sZ_{st}) \\ &= \frac{\mathbf{X}_s\cdot\mathbf{X}_{st}}{\sqrt{R_s^2+Z_s^2}} = \frac{\mathbf{X}_s\cdot\left(\frac{\partial\mathbf{U}}{\partial s}+\frac{\partial\bar{U}}{\partial s}\boldsymbol{\tau}+\bar{U}\frac{\partial\boldsymbol{\tau}}{\partial s}\right)}{\sqrt{R_s^2+Z_s^2}} \\ &= \boldsymbol{\tau}\cdot\left(\frac{\partial\mathbf{U}}{\partial s}+\frac{\partial\bar{U}}{\partial s}\boldsymbol{\tau}+\bar{U}\kappa\mathbf{n}\,|\mathbf{X}_s|\right) = \frac{\partial\mathbf{U}}{\partial s}\cdot\boldsymbol{\tau}+\frac{\partial\bar{U}}{\partial s}. \end{aligned}$$

Substituting the above equality into Eq. (2.16), we obtain

$$\begin{aligned} \frac{\partial\boldsymbol{U}}{\partial s}\cdot\boldsymbol{\tau}+\frac{\partial\bar{U}}{\partial s}(s,t) &= \frac{1}{2\pi}\int_0^{2\pi}\left(\frac{\partial\boldsymbol{U}}{\partial s'}\cdot\boldsymbol{\tau}'+\frac{\partial\bar{U}}{\partial s'}\right)ds' \\ &= \frac{1}{2\pi}\int_0^{2\pi}\frac{\partial\boldsymbol{U}}{\partial s'}\cdot\boldsymbol{\tau}'ds'. \end{aligned} \tag{2.17}$$

Integrating with respect to s, we obtain

$$\bar{U}(s,t)-\bar{U}(0,t) = -\int_0^s \frac{\partial\boldsymbol{U}}{\partial s'}\cdot\boldsymbol{\tau}'ds' + \frac{s}{2\pi}\int_0^{2\pi}\frac{\partial\boldsymbol{U}}{\partial s'}\cdot\boldsymbol{\tau}'ds' \tag{2.18}$$

Let $\bar{U}(0,t)=0$, we obtain the artificial tangential velocity as

$$\bar{U}(s,t)=\frac{s}{2\pi}\int_0^{2\pi}\frac{\partial \boldsymbol{U}}{\partial s'}\cdot\boldsymbol{\tau}'ds'-\int_0^{s}\frac{\partial \boldsymbol{U}}{\partial s'}\cdot\boldsymbol{\tau}'ds' \tag{2.19}$$

By adding the artificial velocity and following the similar derivation as in Eq. (1.13), we have

$$\begin{aligned}\frac{\partial}{\partial t}\left(R|\boldsymbol{X}_s|\right) &= \frac{\partial R}{\partial t}|\boldsymbol{X}_s|+R\frac{\partial|\boldsymbol{X}_s|}{\partial t}\\ &= (U|\boldsymbol{X}_s|+\bar{U}R_s)+R\left(\frac{\partial \boldsymbol{U}}{\partial s}\cdot\boldsymbol{\tau}+\frac{\partial\bar{U}}{\partial s}\right)\\ &= \left(\frac{U}{R}+\frac{\partial \boldsymbol{U}}{\partial \boldsymbol{\tau}}\cdot\boldsymbol{\tau}\right)R|\boldsymbol{X}_s|+\frac{\partial}{\partial s}(\bar{U}R)\\ &= (\nabla_s\cdot\boldsymbol{u})R\,|\boldsymbol{X}_s|+\frac{\partial}{\partial s}(\bar{U}\,R) \qquad (2.20)\end{aligned}$$

It is worth mentioning that another common approach for applying equi-distributed technique is to use a cubic spline interpolation to represent the interface and redistribute the Lagrangian markers uniformly [13]. However, this involves interpolating the surfactant concentration on the interface as well. In the present approach, since the velocity of Lagrangian markers have been modified, the surfactant equation (1.11) must be modified accordingly. Nevertheless, no interpolation is needed in the present approach.

2.1. A modified surfactant equation. By imposing the artificial velocity, the material derivative becomes

$$\frac{D\Gamma}{Dt}=\frac{\partial\Gamma}{\partial t}-(\bar{U}\boldsymbol{\tau})\cdot\nabla\Gamma=\frac{\partial\Gamma}{\partial t}-(\bar{U}\boldsymbol{\tau})\cdot\nabla_s\Gamma=\frac{\partial\Gamma}{\partial t}-\bar{U}\,\frac{\partial\Gamma}{\partial\boldsymbol{\tau}}, \tag{2.21}$$

where the time derivative is taken with respect to fixed s. Substituting the above new material derivative into the surfactant equation (1.11), we thus have

$$\frac{\partial\Gamma}{\partial t}-\bar{U}\,\frac{\partial\Gamma}{\partial\boldsymbol{\tau}}+(\nabla_s\cdot\boldsymbol{u})\,\Gamma=\frac{1}{Pe_s}\,\frac{1}{R|\boldsymbol{X}_s|}\,\frac{\partial}{\partial s}\left(\frac{R}{|\boldsymbol{X}_s|}\,\frac{\partial\Gamma}{\partial s}\right). \tag{2.22}$$

Multiplying both sides by the surface element $R\,|\boldsymbol{X}_s|$ and using the surface divergence identity of Eq. (2.20), we obtain

$$\frac{\partial\Gamma}{\partial t}\,R|\boldsymbol{X}_s|-(\bar{U}\,\frac{\partial\Gamma}{\partial\boldsymbol{\tau}})R|\boldsymbol{X}_s|+\Gamma\left(\frac{\partial}{\partial t}(R|\boldsymbol{X}_s|)-\frac{\partial}{\partial s}(\bar{U}R)\right)=\frac{1}{Pe_s}\,\frac{\partial}{\partial s}\left(\frac{R}{|\boldsymbol{X}_s|}\,\frac{\partial\Gamma}{\partial s}\right).$$

By combining the second and fourth term in above equation, we have

$$\frac{\partial\Gamma}{\partial t}\,R\,|\boldsymbol{X}_s|-\frac{\partial}{\partial s}(R\bar{U}\,\Gamma)+\Gamma\,\frac{\partial}{\partial t}(R\,|\boldsymbol{X}_s|)=\frac{1}{Pe_s}\,\frac{\partial}{\partial s}\left(\frac{R}{|\boldsymbol{X}_s|}\,\frac{\partial\Gamma}{\partial s}\right). \tag{2.23}$$

This is the new modified surfactant equation by taking the artificial tangential velocity of the interface into account. In next section, we shall discretize the above equation to update the surfactant concentration.

3. Numerical method

In this paper, the fluid variables are all defined at the grid center labelled as $\mathbf{x}_{ij}=(r_{i-1/2},z_{j-1/2})=((i-1/2)h,c+(j-1/2)h)$ in Ω, where the grid spacing is uniform in r and z directions. That is, $\Delta r=\Delta z=h$. For the immersed interface, we use a collection of discrete points $s_k=k\Delta s, k=1,2,\ldots,M$ such that the Lagrangian markers are denoted by $\mathbf{X}_k=\mathbf{X}(s_k)=(R_k,Z_k)$. The surfactant concentration Γ_k and surface tension σ_k are defined at the "half-integer" points

given by $s_{k+1/2} = (k+1/2)\Delta s$. Without loss of generality, for any function defined on the interface $\phi(s)$, we approximate the partial derivative $\partial\phi/\partial s$ by

$$D_s\phi\left(s\right) = \frac{\phi\left(s+\Delta s/2\right) - \phi\left(s-\Delta s/2\right)}{\Delta s}. \tag{3.24}$$

Since $|D_s\mathbf{X}_k|$ can approximate the interface stretching factor by using this finite difference convention, the unit tangent vector $\boldsymbol{\tau}_k$ are defined at the "half-integer" points.

Let Δt be the time step size, and n be the superscript time step index. At the beginning of each time step, e.g., step n, the variables $\mathbf{X}_k^n = \mathbf{X}\left(s_k, n\Delta t\right), \Gamma_k^n = \Gamma\left(s_{k+1/2}, n\Delta t\right), \mathbf{u}^n = \mathbf{u}\left(\mathbf{x}, n\Delta t\right)$, and $p^n = p\left(\mathbf{x}, n\Delta t\right)$ are all given. The details of the numerical time integration are as follows.

(1) Compute the surface tension σ_k^n and unit tangent vector $\boldsymbol{\tau}_k^n$ on the interface as

$$\sigma_k^n = \sigma_c\left(1 + \ln\left(1 - \beta\Gamma_k^n\right)\right), \tag{3.25}$$

$$\boldsymbol{\tau}_k^n = \frac{D_s\mathbf{X}_k^n}{|D_s\mathbf{X}_k^n|}, \tag{3.26}$$

both of which hold for $s_{k+1/2} = (k+1/2)\Delta s$. Then we compute the interfacial force as

$$\mathbf{F}_k^n = D_s\left(\sigma_k^n\boldsymbol{\tau}_k^n\right) - \frac{D_s Z_k^n}{R_k^n}\,\sigma_k^n\,\mathbf{n}_k^n, \tag{3.27}$$

at point $\mathbf{X}_k^n$.

(2) Distribute the interfacial force from the markers to the fluid by

$$\mathbf{f}^n\left(\mathbf{x}\right) = \sum_k \mathbf{F}_k^n \delta_h^2\left(\mathbf{x} - \mathbf{X}_k^n\right)\Delta s, \tag{3.28}$$

where the smooth version of two-dimensional Dirac delta function is $\delta_h^2(\mathbf{x}) = d_h(r)\,d_h(z)$, with

$$d_h\left(x\right) = \begin{cases} \frac{1}{4h}\left(1 + \cos\left(\frac{\pi x}{2h}\right)\right), & \text{if } -2h \le x \le 2h \\ 0, & \text{otherwise.} \end{cases} \tag{3.29}$$

(3) Solve the Navier-Stokes equations. This can be done by the following semi-implicit second-order projection scheme, where the nonlinear term is approximated by a second-order extrapolation to avoid solving a nonlinear system at each time step [14].

$$\begin{aligned} &\frac{3\tilde{\mathbf{u}}^{n+1} - 4\mathbf{u}^n + \mathbf{u}^{n-1}}{2\Delta t} + \left(2\left(\mathbf{u}^n\cdot\nabla_h\right)\mathbf{u}^n - \left(\mathbf{u}^{n-1}\cdot\nabla_h\right)\mathbf{u}^{n-1}\right) \\ = \;& -\nabla_h p^n + \frac{1}{Re}\tilde{\Delta}_h\tilde{\mathbf{u}}^{n+1} + \frac{1}{ReCa}\mathbf{f}^n \qquad \tilde{\mathbf{u}} = \mathbf{u}_b, \;\; on\;\partial\Omega \end{aligned} \tag{3.30}$$

$$\tilde{\mathbf{u}}^{n+1} = \mathbf{u}^{n+1} + \frac{2\Delta t}{3}\nabla_h\phi^{n+1} \tag{3.31}$$

$$\tilde{\nabla}_h\cdot\mathbf{u}^{n+1} = 0 \tag{3.32}$$

$$\Delta_h\phi^{n+1} = \frac{3}{2\Delta t}\tilde{\nabla}_h\cdot\tilde{\mathbf{u}}^{n+1} \qquad \nabla_h\phi^{n+1}\cdot\mathbf{n} = 0, \;\; on\;\partial\Omega \tag{3.33}$$

$$p^{n+1} = p^n + \phi^{n+1} - \frac{1}{Re}\tilde{\nabla}_h\cdot\tilde{\mathbf{u}}^{n+1}. \tag{3.34}$$

Here, the discrete gradient operator ∇_h, and the discrete divergence operator $\tilde{\nabla}_h \cdot$ are defined as the standard centered difference approximations to their continuous counterparts as in Eq. (1.6). The discrete Laplace operator Δ_h is also defined as the standard centered difference approximation to the Laplace operator as in Eq. (1.5); thus, the discrete operator $\tilde{\Delta}_h$ in Eq. (3.30) is defined as

$$\tilde{\Delta}_h \tilde{\mathbf{u}}^{n+1} = \left(\Delta_h \tilde{u}^{n+1} - \frac{\tilde{u}^{n+1}}{r^2}, \Delta_h \tilde{w}^{n+1} \right). \tag{3.35}$$

Notice that, due to the axisymmetric property, the boundary conditions for the velocity and the pressure at $r = 0$ are $u = 0$, $\partial w/\partial r = 0$ and $\partial p/\partial r = 0$. One can see that the above Navier-Stokes solver involves solving two Helmholtz equations for the velocity $\tilde{\mathbf{u}}^{n+1}$ and one Poisson equation for the pressure increment ϕ^{n+1}. Those elliptic equations can be solved by using the fast direct solver developed in [10].

(4) Interpolate the new velocity from the fluid lattice points to the marker points, and compute the artificial tangential velocity. Then move the marker points to new positions by using the resultant velocity.

$$\mathbf{U}_k^{n+1} = \sum_{\mathbf{x}} \mathbf{u}^{n+1} \delta_h(\mathbf{x} - \mathbf{X}_k^n) h^2, \tag{3.36}$$

$$\bar{U}_k^{n+1} = \frac{k\Delta s}{2\pi} \sum_{k'=0}^{M} D_s \mathbf{U}_{k'}^{n+1} \cdot \boldsymbol{\tau}_{k'}^n \Delta s - \sum_{k'=0}^{k} D_s \mathbf{U}_{k'}^{n+1} \cdot \boldsymbol{\tau}_{k'}^n \Delta s \tag{3.37}$$

$$\mathbf{X}_k^{n+1} = \mathbf{X}_k^n + \Delta t \mathbf{U}_k^{n+1} + \Delta t \bar{U}_k^{n+1} \boldsymbol{\tau}_k^n. \tag{3.38}$$

(5) Update the surfactant concentration distribution. Since the surfactant is insoluble, the total surfactant mass on the interface must be conserved. It is important to develop a numerical scheme such that the total surfactant mass is preserved numerically. To proceed, as in [11], we discretize Eq. (2.23) by the Crank-Nicholson scheme in a symmetric way as

$$\begin{aligned}
&\frac{\Gamma_k^{n+1} - \Gamma_k^n}{\Delta t} \frac{R_{k+1/2}^{n+1} \left| D_s \mathbf{X}_k^{n+1} \right| + R_{k+1/2}^n \left| D_s \mathbf{X}_k^n \right|}{2} \\
- &\frac{1}{2} \Big[\frac{R_{k+1}^{n+1} \bar{U}_{k+1}^{n+1} \left(\Gamma_{k+1}^{n+1} + \Gamma_k^{n+1} \right)/2 - R_k^{n+1} \bar{U}_k^{n+1} \left(\Gamma_k^{n+1} + \Gamma_{k-1}^{n+1} \right)/2}{\Delta s} \\
+ &\frac{R_{k+1}^n \bar{U}_{k+1}^n \left(\Gamma_{k+1}^n + \Gamma_k^n \right)/2 - R_k^n \bar{U}_k^n \left(\Gamma_k^n + \Gamma_{k-1}^n \right)/2}{\Delta s} \Big] \\
+ &\frac{R_{k+1/2}^{n+1} \left| D_s \mathbf{X}_k^{n+1} \right| - R_{k+1/2}^n \left| D_s \mathbf{X}_k^n \right|}{\Delta t} \frac{\Gamma_k^{n+1} + \Gamma_k^n}{2} \\
= &\frac{1}{Pe_s} \frac{1}{\Delta s} \Big[\frac{R_{k+1}^{n+1}}{|D_s \mathbf{X}_{k+1}^{n+1}| + |D_s \mathbf{X}_k^{n+1}|} \frac{\Gamma_{k+1}^{n+1} - \Gamma_k^{n+1}}{\Delta s} - \frac{R_k^{n+1}}{|D_s \mathbf{X}_k^{n+1}| + |D_s \mathbf{X}_{k-1}^{n+1}|} \frac{\Gamma_k^{n+1} - \Gamma_{k-1}^{n+1}}{\Delta s} \\
+ &\frac{R_{k+1/2}^n}{\left| D_s \mathbf{X}_{k+1}^n \right| + |D_s \mathbf{X}_k^n|} \frac{\Gamma_{k+1}^n - \Gamma_k^n}{\Delta s} - \frac{R_{k-1/2}^n}{|D_s \mathbf{X}_k^n| + \left| D_s \mathbf{X}_{k-1}^n \right|} \frac{\Gamma_k^n - \Gamma_{k-1}^n}{\Delta s} \Big],
\end{aligned} \tag{3.39}$$

where $R_{k+1/2} = (R_{k+1} + R_k)/2$ which is defined at "half-integer" points. Since the new interface marker location $\boldsymbol{X}_k^{n+1}$ is obtained in the previous step, the above discretization results in a tri-diagonal linear system which can be solved easily. More importantly, the total mass of surfactant is

conserved numerically; that is,

$$\sum_k \Gamma_k^{n+1}|D_s\mathbf{X}_k^{n+1}|R_{k+1/2}^{n+1}\Delta s = \sum_k \Gamma_k^n|D_s\mathbf{X}_k^n|R_{k+1/2}^n\Delta s. \tag{3.40}$$

The above equality can be easily derived by taking the summation of both sides of Eq. (3.39) and using the no flux boundary condition of Γ. One should also notice that the summation in Eq. (3.40) is exactly the mid-point rule discretization for the integration of surfactant mass along the interface.

4. Numerical results

In this section, we perform some numerical tests for the scheme developed in previous section. In particular, we check the rate of convergence of our scheme, the comparison of clean (without surfactant) and contaminated (with surfactant) interface with different capillary numbers, the effect of different surface Peclet numbers, and the comparison of linear and nonlinear equation of state.

4.1. Convergence test. Before to proceed, we first carry out the convergence study of the present method. The problem is set up as a freely oscillating drop immersed in a viscous fluid domain $\Omega = [0,1]\times[-1,1]$ which the drop is a spheroid shape with semi-major axis $3/4$ and semi-minor axis $1/3$, respectively. Here, we perform different computations with varying $h = \Delta r = \Delta z = 1/32, 1/64, 1/128, 1/256$. The Lagrangian mesh is chosen as $\Delta s \approx h$ and the time step size is $\Delta t = h/8$. The solutions are computed up to time $t = 1$. We set the Reynolds number $Re = 1$, the capillary number $Ca = 0.25$, and the surface Peclet number $Pe_s = 12.5$. The initial surfactant concentration is uniformly distributed along the interface such as $\Gamma(s,0) = 0.5$. The parameters in Langmuir equation of state (1.10) are chosen as $\sigma_c = 1$ and $\beta = 0.5$, respectively.

Since the analytical solution is not available in these simulations, we choose the results obtained from the finest mesh as our reference solution and compute the L_∞ error between the reference solution and the solution obtained from the coarser grid. Table 1 shows the mesh refinement analysis of the velocity u, w, and the surfactant concentration Γ. One can see that the error decreases substantially when the mesh is refined, and the rate of convergence is somewhat between first and second order. Notice that, the fluid variables are defined at the center of the uniform grid in $r-z$ coordinates and the surfactant concentration is defined at "half-integer" grid, so when we refine the mesh, the numerical solutions will not coincide with the same grid locations. In these runs, we simply use the linear interpolation to compute the solutions at the desired locations. We attribute this is also part of the reason why the rate of convergence behaves less than second-order.

TABLE 1. The mesh refinement analysis of the velocity u, w, and the surfactant concentration Γ.

h	$\|u-u_{ref}\|_\infty$	Rate	$\|w-w_{ref}\|_\infty$	Rate	$\|\Gamma-\Gamma_{ref}\|_\infty$	Rate
1/32	$8.5478E-03$	-	$1.1470E-02$	-	$1.2303E-02$	-
1/64	$2.4752E-03$	1.788	$4.6027E-03$	1.317	$2.4629E-03$	2.321
1/128	$7.5121E-04$	1.720	$1.8433E-03$	1.320	$4.9265E-04$	2.322

4.2. A drop in an extensional flow. In this subsection, we consider a drop in an extensional flow field, $u = -0.5Gr$ and $w = Gz$, where G is the principal strain rate [12] and is chosen as $G = 1$. Throughout the rest of computations, the computational domain is chosen as $\Omega = [0, 1] \times [-4, 4]$, and the parameters in Langmuir equation of state (1.10) are chosen as $\sigma_c = 1$ and $\beta = 0.5$, respectively. We also fix the Reynolds number $Re = 1$ but change the capillary number Ca and the surface Peclet number Pe_s independently to see the effect on a clean (without surfactant) or contaminated (with surfactant) drop elongation. In addition, we will also show the comparison of the results obtained by linear and nonlinear equation of state.

The initial drop is chosen as a circular one with radius $r_0 = 0.3$. For the contaminated interface, the initial surfactant distribution $\Gamma(s, 0) = 0.8$ is used. We use the mesh $h = \Delta r = \Delta z = 1/64$, the Lagrangian mesh $\Delta s \approx h$, and the time step size $\Delta t = h/8$.

4.2.1. A comparison of different capillary number Ca for a drop with or without surfactant. In this example, we compare the effect of different capillary numbers on a clean (without surfactant) or contaminated (with surfactant) drop. Notice that, for the clean case, one do not have to solve the surfactant equation so the surface tension is a constant, i.e. $\sigma = \sigma_c$. It is known that there exists a critical capillary number Ca^* such that the drop is stationary if $Ca < Ca^*$ [3]. Here, the dimensionless capillary number is calculated by $Ca = \frac{\mu G r_0}{\sigma_c}$, where μ is the fluid dynamic viscosity, G is the strain rate, and r_0 is the drop radius. One can also conclude that, the larger capillary number is, the larger elongation of the drop will have. This is because the larger capillary number means the smaller surface tension (by fixing the other parameters), so the drop is easier to elongate. For the contaminated drop case, we choose the surface Peclet number $Pe_s = 18$.

Figure 1 shows the time evolution of a drop in an extensional flow with different capillary numbers. Here, we consider three different cases as follows: (1) clean interface with $Ca = 0.3$: dotted line '..'; (2) clean interface with $Ca = 0.4$: dashed line '–'; (3) contaminated interface with $Ca = 0.3$: solid line '-'. One can see that the clean drop of $Ca = 0.3$ tends to be stationary quickly, while the one of $Ca = 0.4$ elongates slightly as time evolves. However, when the interface is contaminated, the surface tension is reduced significantly so the drop elongates largely. Those numerical results confirm with what we expect as mentioned above.

4.2.2. A comparison of different surface Peclet number Pe_s. In this example, we compare the influence of different surface Peclet number Pe_s on the elongation of contaminated drop. Here, we fix the capillary number as $Ca = 0.3$ and change the surface Peclet number as $Pe_s = 1.8, 18$, and 180. Since the underlying extensional flow drives the surfactant toward to the tips of the drop, the surfactant concentration is higher and thus the surface tension is lower near the tips. When the Peclet number is larger, the surfactant gradient along the interface is larger too, therefore, the overall drop elongation is greater. Figure 2 shows the drop behavior with different Peclet numbers and confirms with what we expect in above. Notice that, the above numerical conclusion is also consistent with the one obtained in [20].

4.2.3. A comparison of the linear and nonlinear equation of state. In this subsection, we use the same set up as in the previous test except that a simplified linear equation of state $\sigma = \sigma_c(1 - \beta\Gamma)$ is also implemented and compared with the results of the nonlinear equation of state. In Figure 3, the evolution of a drop

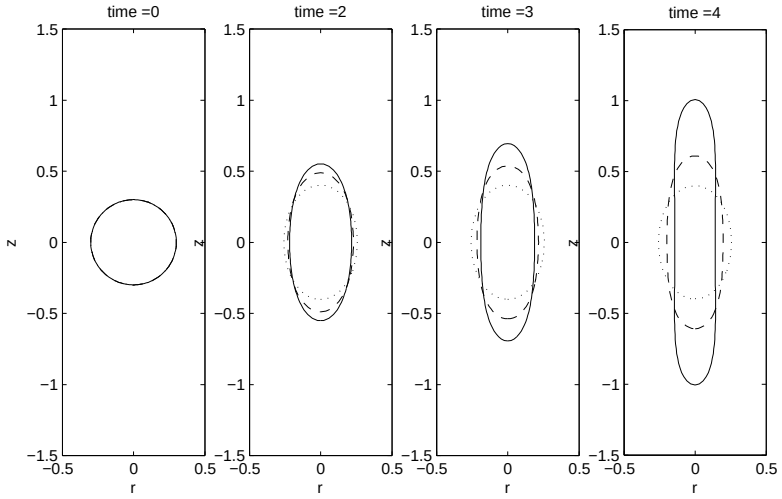

FIGURE 1. The time evolution of a drop in an extensional flow with different capillary numbers. Three different plots are as follows: (1) clean interface with $Ca = 0.3$: dotted line '..'; (2) clean interface with $Ca = 0.4$: dashed line '–'; (3) contaminated interface with $Ca = 0.3$: solid line '-'.

under an extensional flow is shown at different times using the linear and nonlinear equation of states. Our results are consistent with the results obtained in [9], i.e. the drop elongation increases when the nonlinear equation of state is used.

Appendix A. Derivation of the interfacial force

In this appendix, we give a detailed derivation for the interfacial boundary force as shown in Eq. (1.8). As discussed in [17], the singular forcing function $\mathbf{f}$ can be expressed as

$$\mathbf{f}(\mathbf{x}) = -\int_{\Sigma} \Delta\mathbf{T}(\mathbf{x}')\,\delta^3(\mathbf{x}-\mathbf{x}')\,dS(\mathbf{x}'), \tag{A.1}$$

where $\Delta\mathbf{T}$ is the jump in the interface traction, δ^3 is the three-dimensional delta function, and $dS(\mathbf{x}')$ is the surface element. The jump in the interface traction can be derived as

$$\Delta\mathbf{T} = 2\kappa_m\,\sigma\,\mathbf{n} - \nabla_s\sigma, \tag{A.2}$$

where κ_m is the mean curvature of the interface, σ is the surface tension, $\mathbf{n}$ is the unit outward normal defined in (1.1), and ∇_s is the surface gradient operator. In axisymmetric interface, the surface gradient is defined as

$$\nabla_s\sigma = \frac{\partial\sigma}{\partial\boldsymbol{\tau}}\boldsymbol{\tau} = \left(\frac{\partial\sigma}{\partial s}/|\mathbf{X}_s|\right)\boldsymbol{\tau}, \tag{A.3}$$

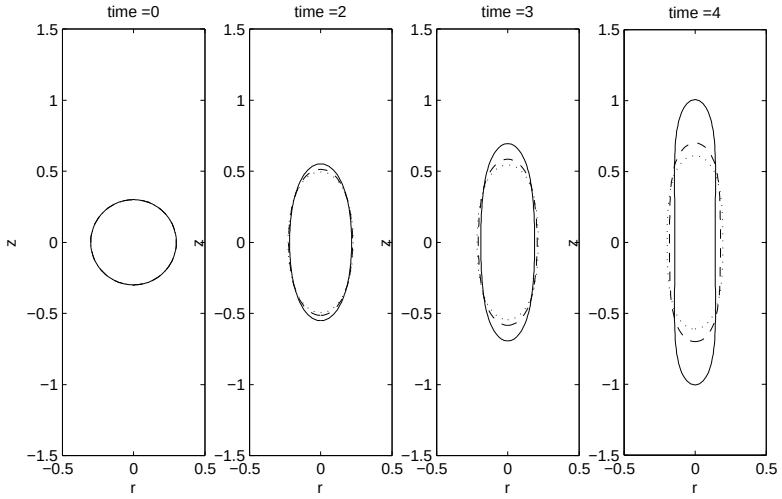

FIGURE 2. The time evolution of a drop in an extensional flow with different surface Peclet numbers. Three different numbers are used: (1) $Pe_s = 1.8$: dotted line '..'; (2) $Pe_s = 18$: dashed line '–'; (3) $Pe_s = 180$: solid line '-'.

where $\boldsymbol{\tau}$ is the unit tangent defined as in Eq. (1.1). One should note that the mean curvature can be found as the surface divergence of the unit normal vector as $2\kappa_m = \nabla_s \cdot \mathbf{n}$. In axisymmetric interface, the surface divergence is obtained in (1.13) so the mean curvature can be calculated as

$$2\kappa_m = \nabla_s \cdot \mathbf{n} = \frac{Z_s}{R|\mathbf{X}_s|} + \left(\frac{\partial \mathbf{n}}{\partial s}/|\mathbf{X}_s|\right) \cdot \boldsymbol{\tau} = \frac{Z_s}{R|\mathbf{X}_s|} + \frac{R_s Z_{ss} - R_{ss} Z_s}{|\mathbf{X}_s|^3}. \tag{A.4}$$

By using those relations in Eqs. (A.3)-(A.4), the interfacial traction can be written as

$$\begin{aligned}
\Delta\mathbf{T} &= \left(\frac{Z_s}{R|\mathbf{X}_s|} + \frac{R_s Z_{ss} - R_{ss} Z_s}{|\mathbf{X}_s|^3}\right) \sigma\, \mathbf{n} - \left(\frac{\partial \sigma}{\partial s}/|\mathbf{X}_s|\right) \boldsymbol{\tau} \\
&= \frac{Z_s}{R|\mathbf{X}_s|}\, \sigma\, \mathbf{n} - \left(\frac{R_{ss} Z_s - R_s Z_{ss}}{|\mathbf{X}_s|^3}\, \sigma\, \mathbf{n} + \frac{1}{|\mathbf{X}_s|}\, \frac{\partial \sigma}{\partial s}\, \boldsymbol{\tau}\right) \\
&= \frac{Z_s}{R|\mathbf{X}_s|}\, \sigma\, \mathbf{n} - \left(\frac{1}{|\mathbf{X}_s|}\, \sigma\, \frac{\partial \boldsymbol{\tau}}{\partial s} + \frac{1}{|\mathbf{X}_s|}\, \frac{\partial \sigma}{\partial s}\, \boldsymbol{\tau}\right) \\
&= \frac{Z_s}{R|\mathbf{X}_s|}\, \sigma\, \mathbf{n} - \frac{1}{|\mathbf{X}_s|}\, \frac{\partial}{\partial s}\, (\sigma \boldsymbol{\tau})\,. \qquad \text{(A.5)}
\end{aligned}$$

By substituting the above traction force into Eq. (A.1) and using the delta function in cylindrical coordinates $\delta^3 = \delta^2/r$ (where δ^2 is the two dimensional delta function

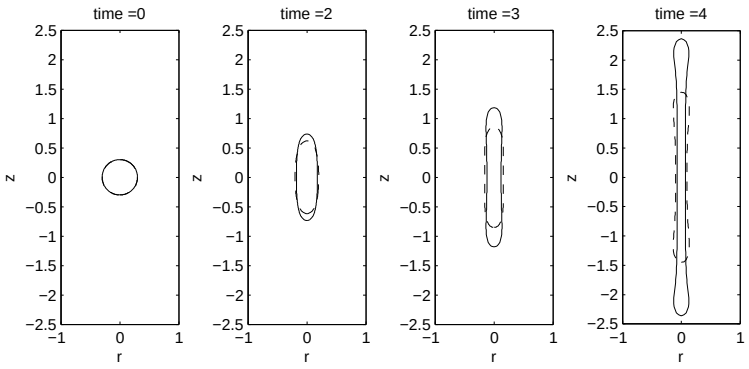

FIGURE 3. The time evolution of a drop in an extensional flow with different equations of state. Here, $Pe_s = 180$ and $Ca = 0.5$. (1) linear EOS: dashed line '–'; (2) nonlinear EOS: solid line '-'.

in r-z plane), we obtain

$$\begin{aligned}\mathbf{f}(\mathbf{x}) &= \int_0^{2\pi} \left(\frac{1}{|\mathbf{X}_s|} \frac{\partial}{\partial s} (\sigma \boldsymbol{\tau}) - \frac{Z_s}{R|\mathbf{X}_s|} \sigma \mathbf{n} \right) \frac{\delta^2(\mathbf{x}-\mathbf{X})}{R} R\,|\mathbf{X}_s|\, ds \\ &= \int_0^{2\pi} \left(\frac{\partial}{\partial s} (\sigma \boldsymbol{\tau}) - \frac{Z_s}{R} \sigma \mathbf{n} \right) \delta^2(\mathbf{x}-\mathbf{X})\, ds.\end{aligned}$$

Therefore, we obtain the interface force $\mathbf{F}$ in Eq. (1.8).

References

[1] A. W. Adamson, *Physical chemistry of surfaces*, John Wiley & Sons, (1976).
[2] G. K. Batchlor, *An introduction to fluid dynamics*, Cambridge University Press, (1967).
[3] J. Blawzdziewicz, V. Cristini, M. Loewenberg, Critical behavior of drops in linear flows. I. Phenomenological theory for drop dynamics near critical stationary states, *Phys. Fluids*, 14 (2002), 2709–2718.
[4] H. D. Ceniceros, The effects of surfactants on the formation and evolution of capillary waves, *Phys. Fluids*, 15(1), (2003) 245–256.
[5] S. Ganesan, L. Tobiska, A coupled arbitrary Lagrangian Eulerian and Lagrangian method for computation of free surface flows with insoluble surfactants, *J. Comput. Phys.*, in press.
[6] P.-G. de Gennes, F. Brochard-Wyart, D. Quere, *Capillarity and wetting phenomena*, Springer, 2003.
[7] M. Hameed, M. Siegel, Y.-N. Young, J. Li, M. R. Booty, D. T. Papageorgiou, Influence of insoluble surfactant on the deformation and breakup of a bubble or thread in a viscous fluid, *J. Fluid Mech.*, 594 (2008), 307–340.
[8] T. Y. Hou, J. S. Lowengrub, M. J. Shelley, Removing the stiffness from interfacial flows with surface tension, *J. Comput. Phys.*, 114 (1994), 312.

[9] A. J. James, J. S. Lowengrub, A surfactant-conserving volume-of-fluid method for interfacial flows with insoluble surfactant, *J. Comput. Phys.*, 201 (2004) 685–722.
[10] M.-C. Lai, W.-W. Lin, W. Wang, A fast spectral/differnce method without pole conditions for Poisson-type equations in cylindrical and spherical geometries, *IMA J. Numer. Anal.*, 22 (2002), 537–548.
[11] M.-C. Lai, Y.-H. Tseng, H. Huang, An immersed boundary method for interfacial flows with insoluble surfactant, *J. Comput. Phys.* 227 (2008), 7279–7293.
[12] J. Li, The effect of an insoluble surfactant on the skin friction of a bubble, *Euro. J. of Mech. B/Fluid*, 25 (2006), 59–73.
[13] Z. Li, K. Ito, *The Immersed Interface Method: Numerical Solutions of PDEs Involving Interfaces and Irregular Domains*, SIAM Frontiers in Applied Mathematics 33, (2006).
[14] J. M. Lopez, J. Shen, An efficient spectral-projection method for the Navier-Stokes equations in cylindrical geometies, I. Axisymmetric cases, *J. Comput. Phys.*, 139 (1998), 308–326.
[15] M. Muradoglu, G. Tryggvason, A front-tracking method for computations of interfacial flows with soluble surfactants, *J. Comput. Phys.*, 227 (2008) 2238–2262.
[16] C. S. Peskin, The immersed boundary method, *Acta Numerica*, 1–39, (2002).
[17] C. Pozrikidis, *Introduction to Theoretical and Computational Fluid Dynamics*, Oxford University Press, (1997), pp 127.
[18] Y. Pawar, K. J. Stebe, Marangoni effects on drop deformation in an extensional flow: the role of surfactant physical chemistry, I. Insoluble surfactants, *Phys. Fluids*, 8 (1996) 1738.
[19] H. A. Stone, A simple derivation of the time-dependent convective-diffusion equation for surfactant transport along a deforming interface, *Phys. Fluids A* 2(1), (1990) 111–112.
[20] H. A. Stone, L. G. Leal, The effects of surfactants on drop deformation and breakup, *J. Fluid Mech.*, 220 (1990), 161–186.
[21] P. Tabeling, *Introduction to Microfluidics*, Oxford University Press, 2005.
[22] H. Wong, D. Rumschitzki and C. Maldarelli, On the surfactant mass balance at a deforming fluid interface, *Phys. Fluids*, 8(11) (1996) 3203–3204.
[23] S. Yon, C. Pozrikidis, A finite-volume/boundary-element method for flow past interfaces in the presence of surfactants, with application to shear flow past a viscous drop, *Comput. Fluids*, 27 (1998), 879–902.
[24] Y.-N. Young, M. R. Booty, M. Siegel, J. Li, Influence of surfactant solubility on the deformation and breakup of a bubble or capillary jet in a viscous fluid, preprint, (2009).
[25] J. Zhang, D. M. Eckmann, P. S. Ayyaswamy, A front-tracking method for a deformable intravascular bubble in a tube with soulble surfactant transport, *J. Comput. Phys.*, 214 (2006) 366–396.

Center of Mathematical Modeling and Scientific Computing & Department of Applied Mathematics, National Chiao Tung University, 1001, Ta Hsueh Road, Hsinchu 300, Taiwan.

E-mail: mclai@math.nctu.edu.tw

URL: http://www.math.nctu.edu.tw/∼mclai/